Ferroelastic and strain glass transition in (1-x)($Bi_{0.5}Na_{0.5}$)TiO_3-x$BaTiO_3$ solid solution

2012 EPL 100 17004

(http://iopscience.iop.org/0295-5075/100/1/17004)

A Letters Journal Exploring the Frontiers of Physics

October 2012

EPL, **100** (2012) 17004
doi: 10.1209/0295-5075/100/17004

www.epljournal.org

Ferroelastic and strain glass transition in (1-x)($Bi_{0.5}Na_{0.5}$)TiO_3-x$BaTiO_3$ solid solution

Yonggang Yao[1], Yaodong Yang[1(a)], Shuai Ren[1,2], Chao Zhou[1], Linglong Li[1] and Xiaobing Ren[1,2(b)]

[1] *Multi-disciplinary Materials Research Center, Frontier Institute of Science and Technology, Xi'an Jiaotong University - Xi'an 710054, China*
[2] *Ferroic Physics Group, National Institute for Materials Science - Tsukuba 305-0047, Ibaraki, Japan*

received 15 June 2012; accepted in final form 6 September 2012
published online 15 October 2012

PACS 77.84.-s – Dielectric, piezoelectric, ferroelectric, and antiferroelectric materials
PACS 77.80.B- – Phase transitions and Curie point

Abstract – The electrical and structure behaviors are somehow deviated in (1-x)($Bi_{0.5}Na_{0.5}$)TiO_3-$x$$BaTiO_3$ (BNT-xBT), which is unusual for regular ferroelectrics whose structure transition is always accompanied with the ferroelectric one. To understand this problem, a dynamic ferroelastic measurement was used as a new way (besides ferroelectric and structure views) to determine its transition. It is found that for $x < 5\%$, they showed a typical ferroelastic phase transition, whereas it was a strain glass transition for $5\% < x < 8\%$ (previously regarded as morphotropic phase boundary region). The new ferroelastic characterization provides a unique aspect to understand complex ferroelectric materials, such as BNT-xBT.

Introduction. – Recently, (1-x)($Bi_{0.5}Na_{0.5}$)TiO_3-$x$$BaTiO_3$ or BNT-xBT attracts lots of research interests as a candidate for Pb free high performance piezoelectric material [1–3]. This material has relatively high Curie temperature and a nearly vertical morphotropic phase boundary (MPB) separating a rhombohedral (R) phase and a tetragonal (T) phase, which (in principle) can generate high piezoelectricity [4–6]. These advantages make it a highly promising substitution material for lead zirconate titanate (PZT) to avoid environmental and health problems.

However, BNT-xBT undergoes a complex phase transition sequence and has complex domain structures, which increases the difficulty to understand its behavior and further optimizing the properties. For example, pure BNT undergoes a transition sequence of R-T and T-C (C as cubic phase) at 300 °C and 540 °C determined by XRD and neutron measurements, and also confirmed by DSC [7–10]. On the other hand, its electrical properties, like ferroelectricity, piezoelectricity and pyroelectricity, encountered a drastic drop around 200 °C and its dielectric peak temperature (T_m) appeared at 320 °C, deviated from the transition temperature determined by these structure measurements [11–15].

Another problem is related to the MPB of BNT-xBT. Relatively large piezoelectricity and permittivity were reported at the MPB, phase boundary between ferroelectric R and T phases [1]. But detailed structure experiments show a pseudo-cubic structure (nearly non-transforming state) for this region from XRD [16], neutron [17] and TEM [18] measurements. These characters do not coincide with those of conventional ferroelectric MPBs which possesses hierarchical domain structure with coexistence of different ferroelectric phases [19].

It is obvious that structure and electrical behaviors of this material are highly divergent, so only viewing from these two aspects cannot solve the above puzzles. A different aspect and new measurements are needed to further understand and clarify these problems. In fact, structure phase transitions are always accompanied with elastic anomalies, and ferroelectric transition has the secondary order parameter as ferroelastic strain ordering, so a ferroelastic study may be a possible way to understand this material, linking the structure transition and its ferroelectric one. Currently, a lot of studies only focused on "ferroelectric BNT-xBT" [2,3], but scarce effort has been made to study the "ferroelastic BNT-xBT" [20], especially no one used the multi-frequency dynamic ferroelastic measurements to characterize this material.

In this work, we used typical ferroelastic characterization methods [21] to study BNT-xBT. We found that

(a) E-mail: yaodongy@mail.xjtu.edu.cn
(b) E-mail: ren.xiaobing@mail.xjtu.edu.cn

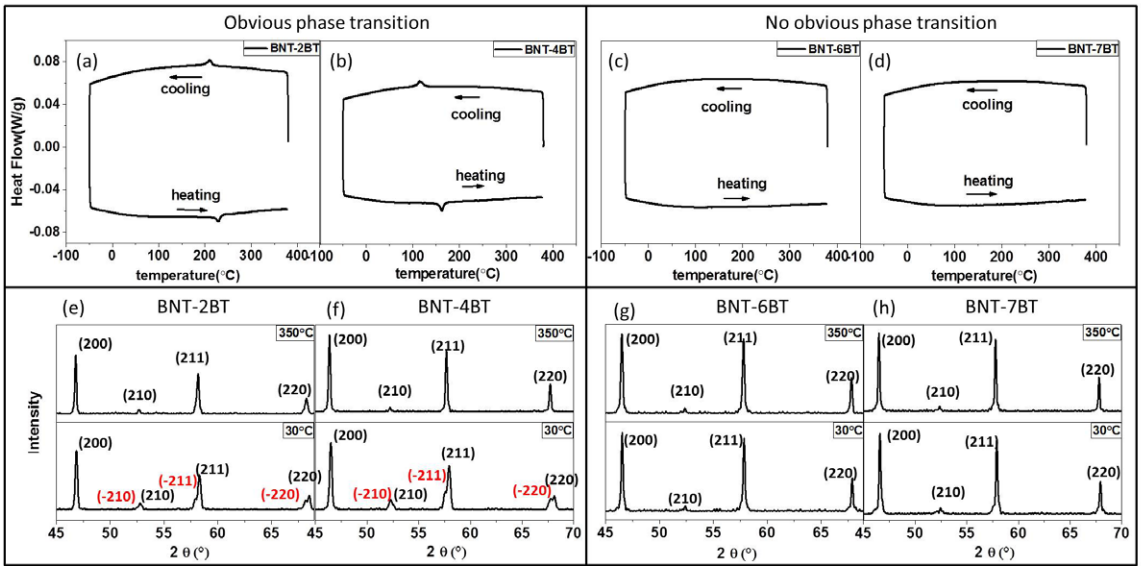

Fig. 1: (Colour on-line) Average structure measurements of BNT-xBT. (a)–(d) DSC heat flows and (e)–(h) XRD profiles at different temperature of BNT-2BT, BNT-4BT, BNT-6BT, and BNT-7BT, respectively.

when $x < 5\%$, it shows a typical ferroelastic transition; but when $5\% < x < 8\%$, BNT-xBT shows a strain glass transition, namely it transits into a frozen short-range order state. (Strain glass is a frozen disordered ferroelastic state with short-range strain order only [22]. It is an important ferroic glass in ferroelastic paralleled to spin glass in ferromagnetic [23] and relaxor in ferroelectric materials [24].) Several puzzles can be explained by adding this ferroelastic viewpoint. These findings provide new information about the transition of BNT-xBT and may lead to new understandings of this material.

Experimental. – Ceramic samples were fabricated with a conventional solid-reaction method. The calcination was performed at 900 °C for 4 h and finally sintered at 1100 °C–1200 °C for 2 h buried in protective powders with the same composition in a sealed crucible. Heat flow was analyzed by DSC-Q200 from TA Instrument. Dynamic mechanical analysis (DMA) and zero-field-cooling or field-cooling (ZFC/FC) strain measurement were done by DMA-Q800 from TA Instrument, too. The structure was analyzed by an X-ray diffraction analysis meter for a temperature range between −100 °C and 350 °C (Shimadzu 7000 XRD).

Results. – Figure 1 shows the transition in BNT-xBT by macro properties measurements of DSC and XRD. Figures 1(a)–(d) are the DSC heat flow curves of BNT-xBT for different compositions. When $x < 5\%$, such as BNT-2BT and BNT-4BT, there are clear exothermic/endothermic peaks during cooling/heating processes, which indicates 1st-order phase transitions. But there are no heat flow peaks in figs. 1(c) and (d), namely no obvious transitions for $5\% < x < 8\%$, such as BNT-6BT and BNT-7BT. These results can be confirmed by XRD line scan, too (figs. 1(e)–(h)). For BNT-2BT and BNT-4BT, there are clear splitting peaks below phase transition temperature indicating a long-range symmetry breaking phase transition (R-like symmetry). While XRD profiles stay the same (pseudo-cubic symmetry) in a wide temperature range for both BNT-6BT and BNT-7BT.

However, DSC and XRD are only effective to observe the long-range phase transition. They are ineffective when used to analysis local order-disorder change for a glass transition: a frozen process from an ergodic state to a nonergodic state with local (short-range) order only [25]. To detect a possible glass transition, new tools are needed, like *ac* magnetic susceptibility measurement for spin glass in ferromagnetic materials [26], permittivity measurement for relaxor in ferroelectric materials [27] and storage modulus measurement for strain glass in ferroelastic materials [22]. Here we use DMA to detect the possible glass state from the ferroelastic aspect. DMA in *ac* mode records the elastic modulus and tangent delta as a function of temperature and frequency. It is effective to reveal the frequency dependence in *ac* modulus and analysis a possible frozen process. DMA in *dc* mode can be used to carry out the zero-field-cooling (ZFC) and field-cooling (FC) experiments with a bias stress field (25 MPa for our experiments). The difference between field-heating (FH) curves after ZFC and FC indicate a history dependence process as well as the loss of ergodicity, which is a primary character of glass transition to show the frozen process [28], similar to the ZFC/FC experiments of relaxor and cluster spin glass [29,30].

Figure 2 shows the temperature-dependent ferroelastic properties measured by DMA. Figures 2(a)–(d) show storage modulus curves and figs. 2(e)–(h) show tangent delta curves in the heating process. For composition $x <$ 5% (figs. 2(a), (b), (e), (f)), the storage modulus and tangent delta show typical ferroelastic transition behaviors

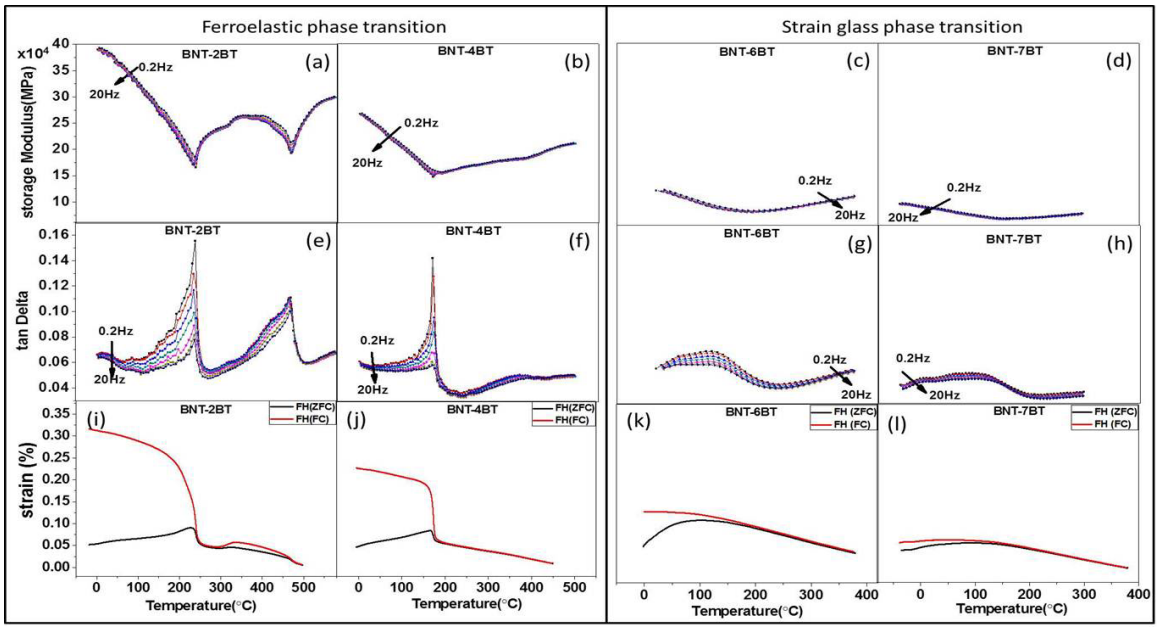

Fig. 2: (Colour on-line) DMA measurement of BNT-xBT. (a)–(d) storage modulus; (e)–(h) tangent delta; (i)–(l) ZFC/FC strain curves with bias stress of 25MPa for BNT-2BT, BNT-4BT, BNT-6BT and BNT-7BT (in a heating process).

with elastic softening on storage modulus and sharp peaks on tangent delta at the phase transition temperature. The frequency independence in the DMA dips/peaks is another important feature of the ferroelastic transition, too. On the other hand, it is very interesting that previous $x > 5\%$ "no-phase-transformation" samples (as revealed by DSC and XRD), now show dips and peaks for modulus and tangent delta in dynamic mechanical measurement, indicating a possible transition (figs. 2(c), (d), (g), (h)). However, the change during transition is much smaller compared with that of the ferroelastic one. The broaden deeps/peaks and the frequency dispersion (see figs. 3(a), (b)) of storage modulus and tangent delta demonstrate a gradual frozen process (strain glass transition) instead of a sharp disorder-order phase transition.

Figures 2(i)–(l) show the ZFC/FC strain curves of BNT-xBT. The ZFC/FC curve usually is used to define the history dependence (or independence) of the material. It is a critical proof to reveal the frozen process of strain glass transition [28–30]. For these samples with composition $x < 5\%$ (figs. 2(i), (j)), after ZFC (zero-field cooling), the spontaneous ordered strain domains are in an isotropic distribution and toll strain is small. But the same samples after the FC (field-cooling) process, the FH (FC) curve starts at a relatively large strain value and decreases gradually with the temperature increasing. When it approaches phase transition temperature, strain decreases quickly and then coincides with the FH (ZFC) curve. This process indicates that after FC, the spontaneous strain is ordered by the bias stress field and formed large ordered strain domains. For $x > 5\%$, the difference between FH curves after ZFC and FC also shows the history dependence and nonergodic process for these samples, indicating the glass

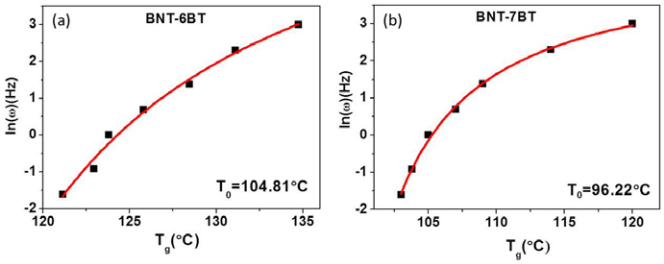

Fig. 3: (Colour on-line) Frequency *vs.* transition temperature curves: (a) BNT-6BT; (b) BNT-7BT (curves are fitting with V-F law).

transition truly happens. However, it should be noticed that the much smaller strain and the gradual mountain shape of the FH (ZFC) curve together are important features of strain glass because strain glass only has nano-sized ordered strain and the randomly frozen domain after ZFC can be excited and re-aligned during the FH process.

The most important feature of a glass transition is its frequency dependence on the transition temperature during an *ac* measurement, which satisfies the Vogel-Fulcher (V-F) relationship [22]. In figs. 3(a) and (b), the frequency dependence of transition temperature T_g (by DMA tan delta measurement) is shown by fitting to the V-F law, and the ideal frozen temperature T_0 (T_g at $f = 0$) was also provided. The glass feature of BNT-6BT and BNT-7BT in mechanical view is clear.

Discussion. – The above data and results revealed the ferroelastic behavior of BNT-xBT. It is shown that for $x < 5\%$, it undergoes a ferroelastic transition, while

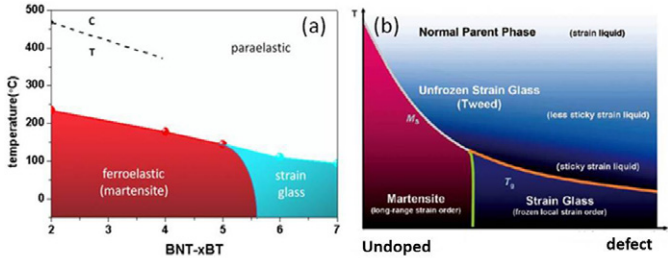

Fig. 4: (Colour on-line) (a) A ferroelastic phase diagram of BNT-xBT system; (b) a typical phase diagram of a strain glass transition [31].

for $5\% < x < 8\%$, it is a strain glass transition. There are four important features for a strain glass transition [21,31]: 1) frequency dependence of *ac* modules (fig. 3); 2) nonergodicity revealed by ZFC/FC curves (fig. 2); 3) no change in the average symmetry by DSC and XRD (fig. 1); 4) existence of a nano-sized domain observed by TEM. Previous works are strongly supportive to verify the domain sizes at different statuses [18,32,33]: When $x < 5\%$, people found relatively large domains (50 to 100 nm), whereas only found a nano-sized domain when $5\% < x < 8\%$. Thus, the existence of strain glass in BNT-xBT for $5\% < x < 8\%$ is clear and assured. (This may be the first strain glass discovered in a ceramic system, also in a ferroelectric material.)

Consequently, the ferroelastic phase diagram of BNT-xBT can be created (fig. 4(a)). It is very similar to the phase diagram of other strain glass materials (fig. 4(b)) [21,31]: with increasing point defect concentration, the ferroelastic transition temperature continually decreases and finally enters into a strain glass state when the defect concentration is beyond a critical value. In BNT-xBT, by doping BT into BNT, the larger Ba^{2+} ions substitute the A site ions (Na^{1+} and Bi^{3+}), then generate random local strains and lattice distortions: Ba^{2+} is regarded as point defect to the ferroelastic transition in this system. With increasing BT concentration, local strains and lattice distortions are increasing, and destroy the long-range strain ordering with the formation of a strain glass state.

It is worth noting that the ferroelastic measurement consists very well with the structure transition. Several "ferroelectric puzzles" can be explained by adding this ferroelastic approach. For example: there is no trace at T_m (the dielectric peak temperature) in ferroelastic measurement (neither in the structure one); namely it cannot be a transition related with structure change or lattice deformation, hence not a typical ferroelectric transition. Some authors proposed it may relate to the superposition relaxation of different kinds of polar nano-regions [34]. Also, as regards the state of "MPB" in BNT-xBT system, though electrical properties enhancement has been found around BNT-6BT, it seems that this composition range is actually a glass state with local order only in ferroelastic view, and simultaneously with a pseudo-cubic structure as previously reported results in XRD [16], neutron [17] and TEM [18] measurement. Finding a strain glass state around the previous MPB region provides strong evidence that this region is a short-range glass state instead of a boundary for two ferroelectric states (for unpoled samples). The details of the relationship between ferroelastic and ferroelectric aspect in BNT-xBT, as well as the origin of the enhancement around BNT-6BT (not a MPB but a glass) will be discussed in another paper.

Strain is considered as a secondary order parameter in ferroelectrics and strain ordering is always accompanied with ferroelectric transitions. Thus, few attention has been paid to the ferroelastic nature of ferroelectric transitions so far. To understand complex ferroelectric systems such as BNT-xBT, a view from ferroelastic aspect actually provides more enlightening information. Clearly, viewing from the ferroelastic side can be another important way to understand a ferroelectric material.

Conclusion. – Ferroelastic and strain glass transitions of BNT-xBT have been studied in this paper. The strain glass state is discovered at composition $5\% < x < 8\%$, which satisfies all the criteria to evaluate a strain glass. Complex ferroelectric transitions and structure puzzles can be well understood if a ferroelastic view is added.

* * *

This work is supported by the Ministry of Science and Technology of China through a 973-Project under Grant No. 2012CB619401 and National Natural Science Foundation of China (Grant No. 11204233).

REFERENCES

[1] Takenaka T., Maruyama K. and Sakata K., *Jpn. J. Appl. Phys. Part 1*, **30** (1991) 2236.
[2] Takenaka T., Nagata H. and Hiruma Y., *Jpn. J. Appl. Phys.*, **47** (2008) 3787.
[3] Rodel J., Jo W., Seifert K. T. P., Anton E.-M., Granzow T. and Damjanovic D., *J. Am. Ceram. Soc.*, **92** (2009) 1153.
[4] Liu W. and Ren X., *Phys. Rev. Lett.*, **103** (2009) 257602.
[5] Damjanovic D., *Appl. Phys. Lett.*, **97** (2010) 062906.
[6] Yao Y., Zhou C., Lv D., Wang D., Wu H., Yang Y. and Ren X., *EPL*, **98** (2012) 27008.
[7] Pronin I. P., Syrnikov P. P., Isupov V. A., Egorov V. M. and Zaitseva N. V., *Ferroelectrics*, **25** (1980) 395.
[8] Zvirgzds J. A., Kapostin P. P., Zvirgzde J. V. and Kruzina T. V., *Ferroelectrics*, **40** (1982) 75.
[9] Park S.-E., Chung S.-J. and Kim I.-T., *J. Am. Ceram. Soc.*, **79** (1996) 1290.
[10] Jones G. O. and Thomas P. A., *Acta Crystallogr. Sect. B*, **58** (2002) 168.
[11] Vakhrushev S. B., Isupov V. A., Kvyatkovsky B. E., Okuneva N. M., Pronin I. P., Smolensky G. A. and Syrnikov P. P., *Ferroelectrics*, **63** (1985) 153.
[12] Suchanicz J., *Ferroelectrics*, **190** (1997) 77.
[13] Suchanicz J., *Ferroelectrics*, **209** (1998) 561.

[14] Roleder K., Franke I., Glazer A. M., Thomas P. A., Miga S. and Suchanicz J., *J. Phys.: Condens. Matter*, **14** (2002) 5399.
[15] Dorcet V. and Trolliard G., *Acta Mater.*, **56** (2008) 1753.
[16] Ranjan R. and Dviwedi A., *Solid State Commun.*, **135** (2005) 394.
[17] Simons H., Daniels J., Jo W., Dittmer R., Studer A., Avdeev M., Rodel J. and Hoffman M., *Appl. Phys. Lett.*, **98** (2011) 082901.
[18] Ma C., Tan X., Dul'kin E. and Roth M., *J. Appl. Phys.*, **108** (2010) 104105.
[19] Gao J., Xue D., Wang Y., Wang D., Zhang L., Wu H., Guo S., Bao H., Zhou C., Liu W., Hou S., Xiao G. and Ren X., *Appl. Phys. Lett.*, **99** (2011) 092901.
[20] Cordero F., Craciun F., Trequattrini F., Mercadelli E. and Galassi C., *Phys. Rev. B*, **81** (2010) 144124.
[21] Ren X., Wang Y., Otsuka K., Lloveras P., Castan T., Porta M., Planes A. and Saxena A., *MRS Bull.*, **34** (2009) 838.
[22] Sarkar S., Ren X. and Otsuka K., *Phys. Rev. Lett.*, **95** (2005) 205702.
[23] Fischer K. and Hertz J., *Spin Glasses*, Vol. **1** (Cambridge University Press) 1993.
[24] Cross L. E., *Ferroelectrics*, **76** (1987) 241.
[25] Angell C. A., *Science*, **267** (1995) 1924.
[26] Snyder J., Slusky J. S., Cava R. J. and Schiffer P., *Nature*, **413** (2001) 48.
[27] Vugmeister B. E. and Glinchuk M. D., *Rev. Mod. Phys.*, **62** (1990) 993.
[28] Wang Y., Ren X., Otsuka K. and Saxena A., *Phys. Rev. B*, **76** (2007) 132201.
[29] Viehland D., Jang S. J., Cross E. and Wuttig M., *Philos. Mag. A*, **64** (1991) 835.
[30] Gayathri N., Raychaudhuri A., Tiwary S., Gundakaram R., Arulraj A. and Rao C., *Phys. Rev. B*, **56** (1997) 1345.
[31] Ren X., Wang Y., Zhou Y., Zhang Z., Wang D., Fan G., Otsuka K., Suzuki T., Ji Y., Zhang J., Tian Y., Hou S. and Ding X., *Philos. Mag.*, **90** (2010) 141.
[32] Soukhojak A. N., Wang H., Farrey G. W. and Chiang Y. M., *J. Phys. Chem. Solids*, **61** (2000) 301.
[33] Yao J., Monsegue N., Murayama M., Leng W., Reynolds W. T., Zhang Q., Luo H., Li J., Ge W. and Viehland D., *Appl. Phys. Lett.*, **100** (2012) 012901.
[34] Jo W., Schaab S., Sapper E., Schmitt L. A., Kleebe H.-J., Bell A. J. and Roedel J., *J. Appl. Phys.*, **110** (2011) 074106.